IEEE Access
Multidisciplinary ⋮ Rapid Review ⋮ Open Access Journal

Received March 2, 2020, accepted March 16, 2020, date of publication March 19, 2020, date of current version March 30, 2020.

Digital Object Identifier 10.1109/ACCESS.2020.2981944

Multilevel Image Dehazing Algorithm Using Conditional Generative Adversarial Networks

KAILEI GAN, JIEYU ZHAO, AND HAO CHEN
Faculty of Electrical Engineering and Computer Science, Ningbo University, Ningbo 315211, China

Corresponding author: Jieyu Zhao (zhao_jieyu@nbu.edu.cn)

This work was supported in part by the National Natural Science Foundation of China under Grant 61571247, in part by the Zhejiang Provincial Natural Science Foundation of China under Grant LZ16F030001, and in part by the K. C. Wong Magna Fund of Ningbo University.

ABSTRACT In recent years, the hazy weather in China occurs frequently, and image dehazing has gradually become a research hotspot. To improve the dehazing effect of the hazy images, this paper has proposed a multilevel image dehazing algorithm using conditional generative adversarial networks (CGAN). The hazy image is used to generate the composed image K jointly estimated by a transmission map and atmospheric light value through a generator network, and a dehazed image is calculated through an improved atmospheric scattering model. The generator network and the joint discriminator network are subjected to adversarial training and reconstruction constraints. The experimental results show that the proposed method achieved good dehazing effect in synthetic hazy images and real hazy images, and is ahead of other advanced dehazing methods in subjective evaluation and objective evaluation.

INDEX TERMS CGAN, jointly estimate, atmospheric scattering model, image dehazing.

I. INTRODUCTION

Hazy weather reduces the color saturation and contrast in images, and many image details are lost. In addition, such weather greatly affects the fields of satellite remote sensing monitoring, target recognition and tracking, and traffic monitoring. Therefore, image dehazing has very important practical application value and research significance.

The purpose of image dehazing is to reduce or remove the effect of haze for more effective subsequent research. In recent years, there have been many studies on image dehazing [1]–[6]. He *et al.* [7] proposed a dark channel prior method, which achieved good dehazing effects, but the soft matting method used had problems of low efficiency and a large number of calculations. Subsequently, He *et al.* [8] proposed using guided filtering instead of soft matting, which not only increased the accuracy of transmission image estimation but also improved the calculation efficiency. However, the dehazed image is generally dark and prone to distortion when there is a large area of sky. Ancuti and Ancuti [9] proposed a fusion-based method that fuses two images with enhanced contrast and white balance through a multiscale Laplacian pyramid. This can preserve the long-range and close-up information of the image, but it is also possible to fuse defects in the image, which affects the dehazing results. Berman *et al.* [10] proposed a hazy line-based method to estimate the transmission map through the hazy line. This method has high calculation efficiency, but when the scene brightness is lower than the atmospheric light, it is more difficult to detect the hazy line, which reduces the estimation accuracy of the transmission map. Although the effect of the traditional dehazing method has been greatly improved, most methods rely too much on a priori information, making the dehazing results less than ideal in actual situations.

Due to the rapid development of deep learning, an increasing number of researchers have applied deep learning methods to image dehazing, which can reduce dependence on prior information. Cai *et al.* [11] used a convolutional neural network (CNN) to estimate transmission maps in image dehazing, and extracted multiscale features by using filters of different scales in the network structure, and obtained better dehazing results. Ren *et al.* [12] proposed a multilevel CNN for estimating transmission maps. This network contains two subnetworks, one for estimating coarse-grained transmission maps and the other for estimating fine-grained transmission maps, so that more detailed transmission maps can be obtained. However, since the abovementioned deep learning-based dehazing methods use operations such as maximum pooling, it is easy to lose some details when

The associate editor coordinating the review of this manuscript and approving it for publication was Fan Zhang.

learning to generate a transmission map, thereby affecting the result of image dehazing.

Because the above methods cause cumulative error when estimating the intermediate parameters of the physical model step by step, Li *et al.* [13] performed end-to-end image dehazing through CGAN [14] and directly learned the mapping relationship between the hazy image and the dehazed image. However, there are still cases where the image details are lost, and the dehazing is incomplete. Engin *et al.* [15] proposed using a cycle-consistent generation adversarial network (CycleGAN) for end-to-end image dehazing, but there are still considerable residual haze and low definition in the dehazed image.

To reduce the cumulative error caused by multiple intermediate parameters and increase the detailed information of the image, this paper proposes a multilevel image dehazing algorithm using CGAN. First, the transmission map and the atmospheric light value are jointly estimated; that is, the transmission map and the atmospheric light value are unified into the image K [16]. Second, using CGAN as a training framework, a structural similarity index measure (SSIM) [17] is added to the loss function of the generator network to increase image detail. Finally, the hazy image is generated into image K by the generator network, and then the improved atmospheric scattering model is used to obtain the dehazed image. The generator network and the joint discriminator network are subjected to adversarial training and reconstruction constraints, and finally an end-to-end dehazing model is obtained. Compared with other advanced dehazing methods, the proposed method can obtain a better dehazing effect.

The main contributions of this paper are as follows:

- We propose a new end-to-end dehazing network. This network uses CGAN framework and atmospheric scattering model.
- To generate better dehazed results, we use U-Net to generate image K which is jointly estimated by transmission map and atmospheric light value. And dehazed image is obtained by the improved atmospheric scattering model. Besides, training the whole network through CGAN.
- This paper compares the synthetic hazy image test set and the real hazy image test set with a variety of advanced image dehazing methods to evaluate the performance. In addition, an ablation study is conducted to demonstrate the influence of k and loss functions on dehazing results.

II. RELATED WORK

A. ATMOSPHERIC SCATTERING MODEL

The purpose of image dehazing is to recover a clear dehazed image from a hazy image. This process can be formulated by [18], [19]

$$I(x) = J(x)t(x) + A(1 - t(x)) \tag{1}$$

where I represents a hazy image, J represents a dehazed image, A represents an atmospheric light value, t represents a transmission map, and x represents index image pixels. $J\ (x)t\ (x)$ is the direct attenuation term, which represents the part of the imaging system after the attenuation of the reflected light transmission in the scene; and $A(1 - t(x))$ is the atmospheric light term, which represents the effect of the intensity of light received at the observation point with the ambient light under the atmosphere. Assuming that the atmosphere medium is homogeneous and uniform, the expression of the transmission map is as follows:

$$t(x) = e^{-\beta d(x)} \tag{2}$$

where d represents the distance between the scene point and the camera, and β represents the atmospheric scattering coefficient.

The atmospheric scattering model is analyzed and derived, and the atmospheric light value A and the transmission map t in the model are unified into a variable K, and the expression is as follows:

$$\begin{aligned} J(x) &= \frac{1}{t(x)} I(x) - A\frac{1}{t(x)} + A \\ &= K(x)I(x) - K(x) + b \end{aligned} \tag{3}$$

$$K(x) = \frac{\frac{1}{t(x)}(I(x) - A) + (A - b)}{I(x) - 1} \tag{4}$$

where b is a constant deviation with a default value of 1.

B. CONDITIONAL GENERATIVE ADVERSARIAL NETWORK

Conditional generative adversarial network (CGAN) is different from generative adversarial networks (GAN) [20]. It carries the condition information y and introduces the condition information y into generator network G and discriminator network D. This condition information y can be based on a variety of information, such as image information, label information, or other modal data. In the generator network G, random noise z and condition information y constitute a new joint hidden layer representation. The objective function of CGAN is a minimax game with conditional probability. The objective function $V\ (G, D)$ can be expressed as:

$$\begin{aligned} \min_G \max_D V(G, D) = {} & E_{x\sim P_{data}(x)}[\log D(x|y)] \\ & + E_{z\sim P_{rose}(x)}[\log(1 - D(G(z|y)))] \end{aligned} \tag{5}$$

where $P_{data}(x)$ represents the distribution of real samples, $P_{noise}(x)$ represents the distribution of random noise, and E $(\cdot)$ represents the expected value of calculation.

Apply formula (5) to image dehazing, so that the random noise z and the input hazy image I generate image K by generator network G, and the dehazing image J obtained by formula (3) is added to the input of joint discriminator network D_j. This process can be formulated as

$$\begin{aligned} \min_G \max_{D_j} V\left(G, D_j\right) = {} & E_{I,K_r,J}\left[\log D_j\left(I, K_r, J_r\right)\right] \\ & + E_{I,z}\left[\log\left(1 - D_j(I, G(I, z), J)\right)\right] \end{aligned} \tag{6}$$

where $G(I, z)$ represents the generated image K, K_r represents the label image of the generated image K, and

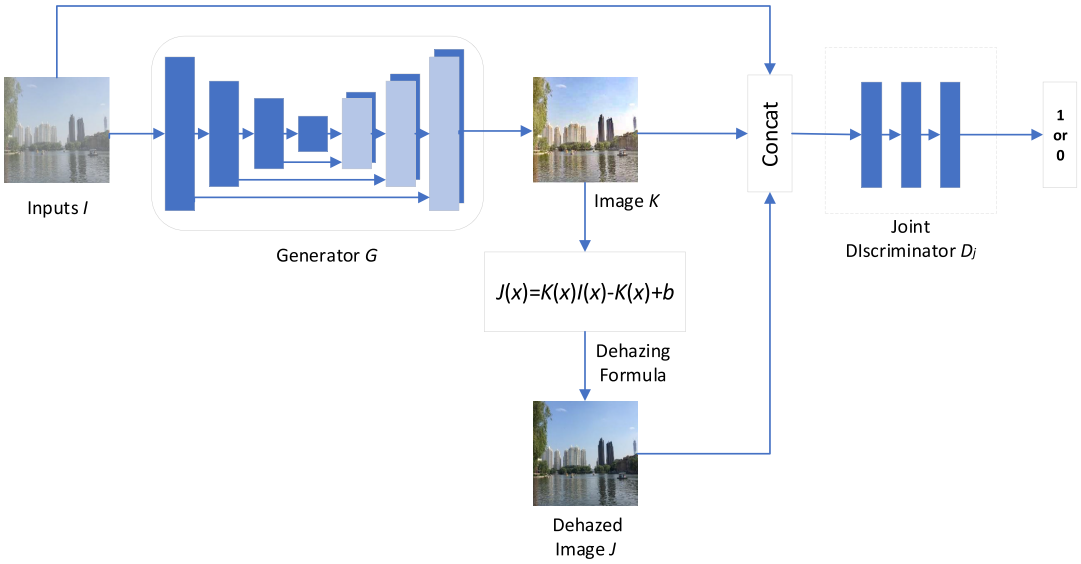

FIGURE 1. Multilevel image dehazing using conditional generative adversarial networks.

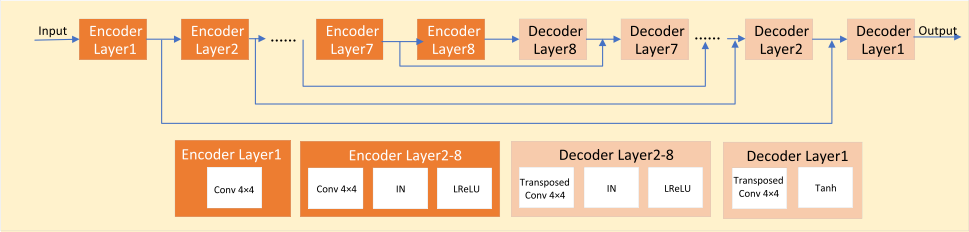

FIGURE 2. Generator network structure.

J_r represents the label image of the generated dehazed image J.

III. PROPOSED METHOD

The network structure used in this paper is shown in Figure 1. First, the hazy image I generates an image K through a generator network G, then the image K generates a dehazed image J through an improved atmospheric scattering model, and finally the discrimination is performed by a joint discriminator network D_j. In this paper, CGAN is used as the training framework, and SSIM is used as the loss function, which improves the effect of image dehazing.

A. GENERATOR NETWORK

The function of the generator network G is to convert the input hazy image I into an image K. For such a specific image-to-image conversion problem, there are a large number of low-level features between the input image and the output image. For example, the input and output images of this generator network share the edge position and protruding structure. This paper uses the U-Net structure [21]. This network connects the encoder to the decoder through a residual connection so that the decoder can better repair the details of the target image. The function of each residual connection is to connect all channels at the encoder layer i and the decoder layer i, where i is the number of layers.

The structure of the generator network G is shown in Figure 2, where "tanh" represents the tanh activation function, "LReLU" represents the Leaky ReLU activation function, "IN" represents instance normalization, "conv" represents convolution.

B. JOINT DISCRIMINATOR NETWORK

The input of the joint discriminator network D_j is different from the input of the general discriminator network. It is a joint input with condition information, in which the hazy image I is its condition information. The input of the joint discriminator network D_j is the combination of the generated image K, the dehazed image J, and the hazy image I, or the combination of the label image K_r, the label image J_r, and the hazy image I, which is similar to an image with 9 channels. The goal of the joint discriminant network D_j is to separately identify these two parts, so that the probability of the former output through the joint discriminator network D_j approaches 0, and the probability of the latter output through the joint discriminator network D_j approaches 1.

The structure of the joint discriminator network D_j is shown in Figure 3. The first to fourth convolution layers are

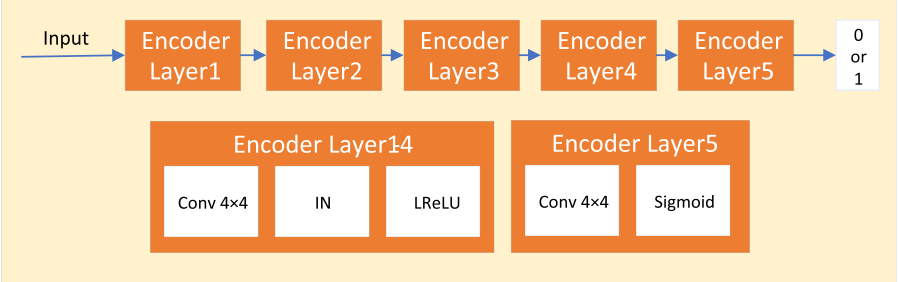

FIGURE 3. Joint discriminator network structure.

connected to IN layer and LReLU activation function layer, and the last convolution layer is connected to the sigmoid activation function. In addition, the sizes of the convolution filters are all 4×4.

C. LOSS FUNCTION

The loss functions of the generator network G and the joint discriminator network D_j are respectively introduced as follows.

The loss function of the generator network G consists of three losses. The first one is the adversarial loss L_a of the joint discriminator network D_j. The second is L_{SSIM} which is the sum of the SSIM losses of the image K and its label image K_r and the dehazed image J and its label image J_r. The third is $L1^*$ which is the sum of the $L1$ losses of the image K and its label image K_r and the dehazed image J and its label image J_r.

The adversarial loss L_a is the most important loss in adversarial learning. It comes from the discrimination result of the joint discriminator network D_j. If the generated image K and the dehazed image J are more different from their label images, the discriminant accuracy of the joint discriminator network Dj for its joint input is higher. It can be seen that the judgment accuracy of the joint discriminator network D_j for the joint input is opposite to the adversarial loss L_a. The adversarial loss L_a can be expressed as:

$$L_a = \log\left(1 - D_j(I, K, J)\right) \tag{7}$$

The loss L_{SSIM} is the sum of SSIM losses where SSIM is similar to the human visual system (HVS). Using SSIM as a loss function can increase image details. SSIM is defined as:

$$\mathrm{SSIM}(x, y) = \frac{\left(2\mu_x\mu_y + C_1\right)\left(\sigma_{xy} + C_2\right)}{\left(\mu_x^2 + \mu_y^2 + C_1\right)\left(\sigma_x^2 + \sigma_y^2 + C_2\right)} \tag{8}$$

where μ_x represents the average of x, μ_y represents the average of y, σ_x represents the standard deviation of x, σ_y represents the standard deviation of y, and σ_{xy} represents the covariance of x and y. C_1 and C_2 are constants set to avoid the denominator being 0. Usually, $C_1 = (K_1 * T)^2$ and $C_2 = (K_2 * T)^2$. Generally, $K_1 = 0.01$, $K_2 = 0.03$, and T is the dynamic range of pixel values.

DSSIM is a distance measure based on SSIM

$$DSSIM = \frac{1 - SSIM(x, y)}{2} \tag{9}$$

Therefore, L_{SSIM} which is the sum of SSIM losses can be expressed as:

$$L_{SSIM} = DSSIM(K, Kr) + DSSIM(J, Jr) \tag{10}$$

The loss $L1^*$ is the sum of $L1$ losses and can be expressed as:

$$\begin{aligned} L1^* &= L1(K) + L1(J) \\ &= E\left[\|K_r - K\|_1\right] \\ &\quad + E\left[\|J_r - J\|_1\right] \end{aligned} \tag{11}$$

Therefore, the overall loss function L_G of the generator network G can be expressed as:

$$L_G = \lambda_1 L_a + \lambda_2 L_{SSIW} + \lambda_3 L1^* \tag{12}$$

where λ_1, λ_2, and λ_3 represent the proportion of each partial loss function to the overall loss function.

The joint discriminator network D_j is essentially a classification network, and its loss function L_D can be expressed as:

$$L_D = \log\left(D_j(I, K_r, J_r)\right) + \log\left(1 - D_j(I, K, J)\right) \tag{13}$$

The overall optimization goal of the proposed method is to minimize the loss function of the generator network G and maximize the loss function of the joint discriminator network D_j, which can give the dehazed image a better dehazing effect.

IV. EXPERIMENTAL RESULTS AND ANALYSIS

This paper compares the synthetic hazy image test set and the real hazy image test set with a variety of advanced image dehazing methods to evaluate the performance. The methods selected for comparison, includeing He method [8], Engin method [15], Li method [13], and Li method [16], where He method [8] is based on the dark channel prior, Engin method [15] is based on the CycleGAN, Li method [13] is based on the CGAN, and Li method [16] is based on the convolutional neural network (CNN). To compare the effects of K and loss functions on the method, comparison experiments on the synthetic hazy image test set are performed.

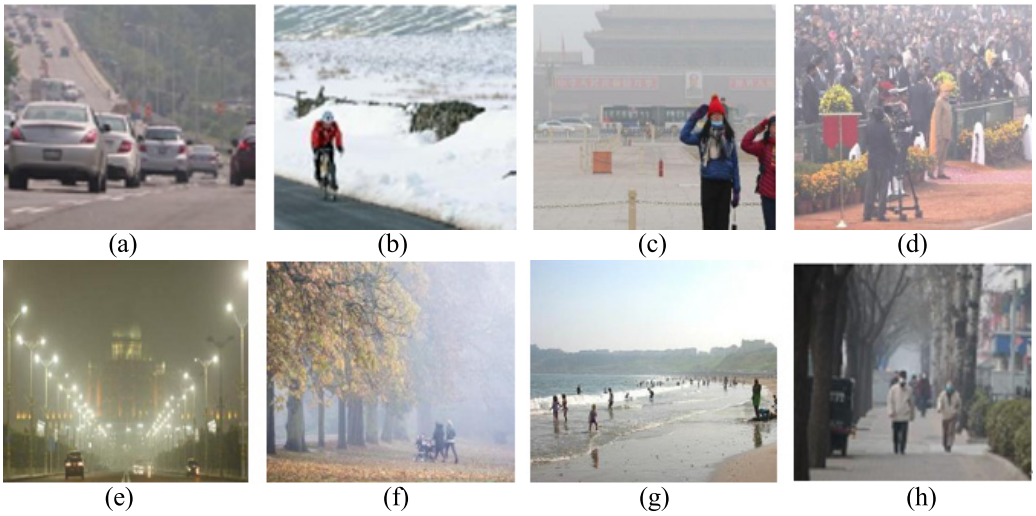

FIGURE 4. Real hazy images for testing. (a) Traffic. (b) Winter. (c) Architecture. (d) Crowd. (e) Night. (f) Plant. (g) Beach. (h) Street.

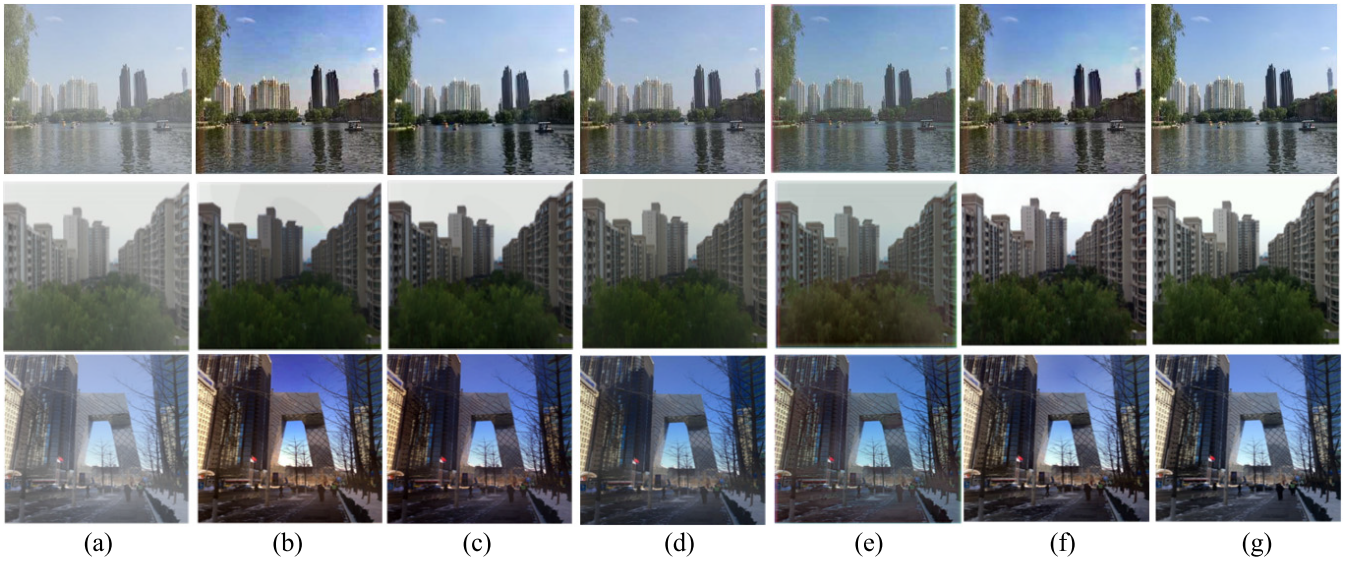

FIGURE 5. Dehazed results of the synthetic hazy image test set. (a) Inputs. (b) He method [8]. (c) Engin method [15]. (d) Li method [13]. (e) Li method [16]. (f) Proposed method. (g) Ground truth.

A. EXPERIMENTAL SETUP

Dataset: in this paper, 8,000 label image K_r - label image J_r - hazy image I image pairs are training set. The label image J_r in this training sets comes from the RESIDE data set [22] and the Middlebuty data set [23]. The hazy image I and the label image K_r are generated as follows: let each label image J_r randomly set the atmospheric scattering coefficient β and the global atmospheric light value A, where $\beta \in [0.8,1.6]$, $A \in [0.8,1.0]$, and then calculate the hazy image I according to formula (1) and formula (2), and then according to formula (4), the label image K_r can be obtained. In addition, another 800 synthetic hazy images are test set. Then, to test the dehazing effect of the method on the real hazy image, 8 real hazy images are randomly selected as the real hazy image test set to test the dehazing effect in different scenes, including traffic, winter and buildings, as shown in Figure 4.

Parameter setting: this method is based on TensorFlow 1.8 deep learning framework, and uses a GPU to speed up the operation. The optimization of the network adopts the improved Adam algorithm. The size of the batch processing is 4, the initial learning rate is set to 0.0002, the training round is 100, the learning rate of the first 50 rounds remains unchanged, and the learning rate of the last 50 rounds decreases linearly to 0.

B. SUBJECTIVE EVALUATION OF DEHAZING METHODS

As shown in Figure 5, for the synthetic hazy images, the overall color of the dehazed image obtained by He method [8]

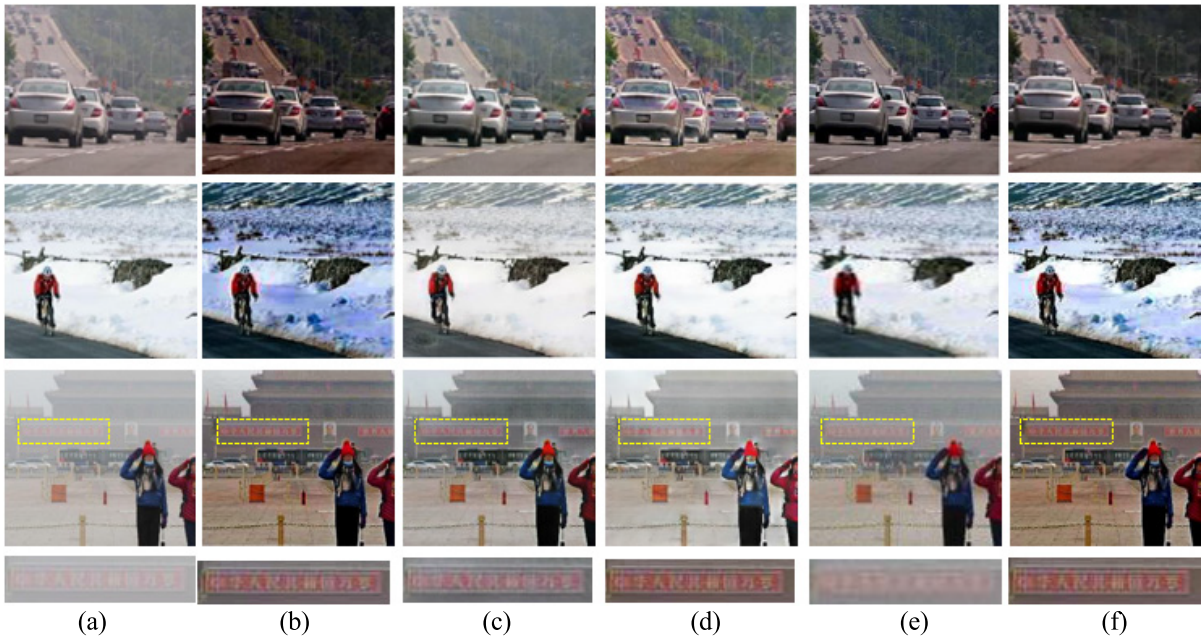

FIGURE 6. Dehazed results of real hazy image test set. (a) Inputs. (b) He method [8]. (c) Engin method [15]. (d) Li method [13]. (e) Li method [16]. (f) Proposed method.

TABLE 1. Objective evaluation of dehazed results in synthetic hazy image test set.

Method	Inputs	He method [8]	Engin method [15]	Li method [13]	Li method [16]	Proposed method
PSNR	15.4335	19.8583	21.1036	28.6229	23.5698	**29.9542**
SSIM	0.7852	0.8671	0.8536	0.8987	0.8815	**0.9147**
IE	7.0966	7.2172	7.2892	7.3111	7.3261	**7.3833**
AG	6.9626	7.2411	7.1561	7.3694	7.2873	**7.6952**

TABLE 2. IE of different methods in real hazy images.

Method	Inputs	He method [8]	Engin method [15]	Li method [13]	Li method [16]	Proposed method
Traffic	6.9729	7.1393	7.2648	7.3683	7.3712	**7.4417**
Winter	7.1008	**7.6742**	7.1495	7.3221	7.1231	7.5796
Architecture	7.0081	7.4245	7.2825	7.3596	7.1679	**7.6636**
Crowd	6.5493	6.7192	6.8545	6.8863	6.6643	**6.9947**
Night	6.5569	6.6132	7.2632	**7.3021**	6.7667	6.8338
Plant	7.1376	7.3482	7.4784	7.5364	7.2836	**7.6325**
Beach	6.8902	7.2213	7.1783	7.2136	6.9761	**7.4562**
Street	6.1688	6.4172	6.2626	6.3728	6.5678	**6.7074**
Average Results	6.7980	7.0696	7.0917	7.1701	6.9901	**7.2886**

is darker, and there is color distortion in the sky area, which is slightly excessive dehazing. Some areas of the dehazed image obtained by Engin method [15] and Li method [13] leave a certain amount of residual hazy, which is not enough to dehaze. The dehazed image obtained by Li method [16] is color distortion on the whole. The dehazed image obtained by the proposed method looks clearer and more natural overall, and has more details, no color deviation and is more similar to the original image.

TABLE 3. AG of different methods in real hazy images.

Method	Inputs	He method [8]	Engin method [15]	Li method [13]	Li method [16]	Proposed method
Traffic	6.7489	7.8401	9.1015	9.6587	9.3698	**10.0092**
Winter	8.2021	**12.0446**	9.5288	10.8358	9.4175	11.6455
Architecture	6.3566	7.3674	7.2597	7.8367	7.4216	**8.1724**
Crowd	6.8382	7.3665	7.1809	7.5256	6.9882	**7.7756**
Night	3.4545	5.2609	6.4584	**6.9627**	6.5963	5.8951
Plant	7.0829	9.9606	9.6024	10.3152	9.4671	**11.2049**
Beach	5.2557	8.2147	7.7967	8.0952	7.3695	**9.9795**
Street	7.1324	8.2205	8.0983	8.3496	8.5167	**8.8987**
Average Results	6.3839	8.2844	8.1283	8.6974	8.1433	**9.1976**

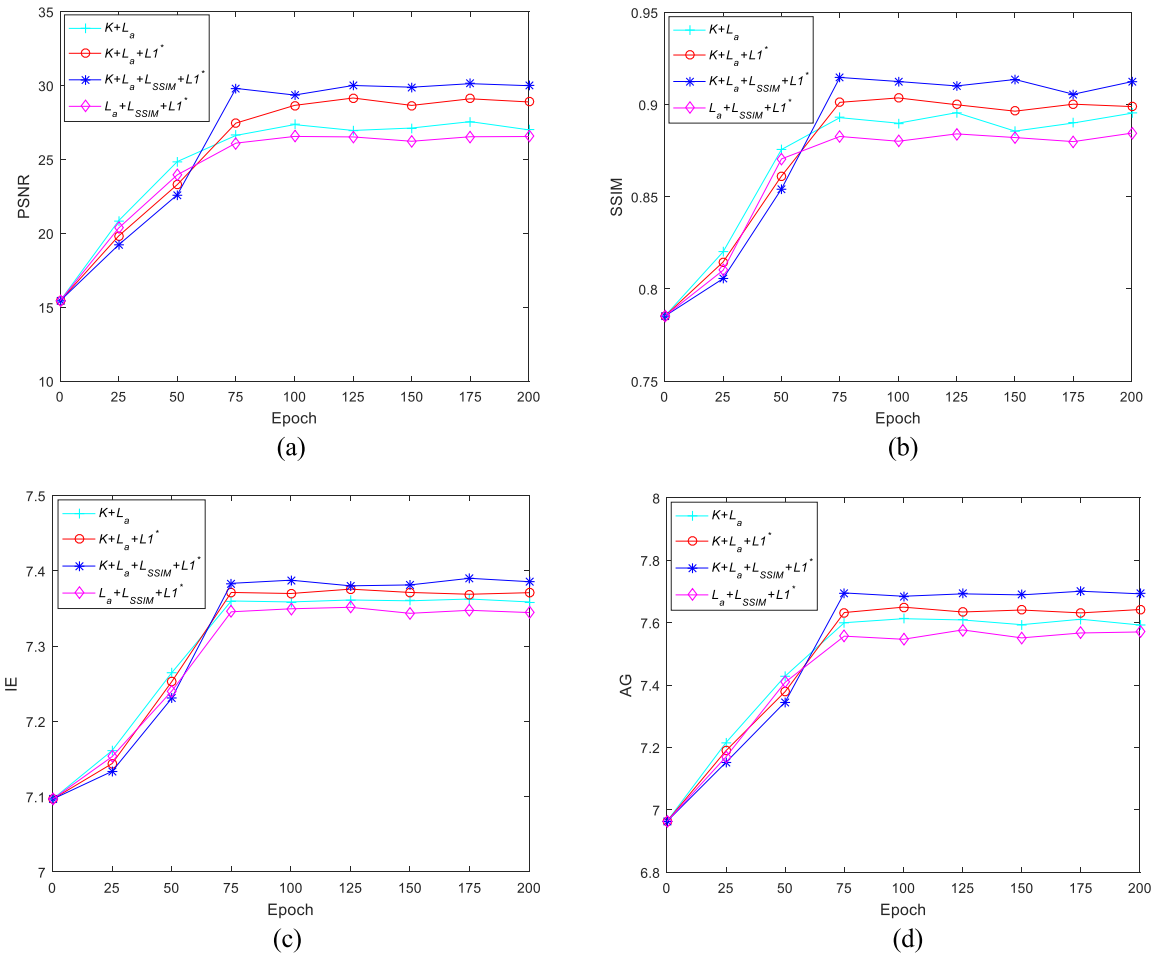

FIGURE 7. Influence of k and loss functions on dehazing results. (a) PSNR. (b) SSIM. (c) IE. (d) AG.

As shown in Figure 6, for the real hazy images, the dehazed image obtained by He method [8] is fuzzy and not obvious in the details, and the color distortion still appears in the sky area. The dehazed images obtained by Engin method [15] and Li method [13] have more residual haze and dehaze incompletely at a deeper depth of field, and the improvement of image clarity and contrast is small. The dehazed image obtained by Li method [16] is a little fuzzy on the whole. The dehazed image obtained by the proposed method has less haze and the image color is more natural. In addition,

the enlarged patches of the dehazed results obtained by the proposed method are clearer, the detail information is more complete, and the dehazing is more thorough.

C. OBJECTIVE EVALUATION OF DAHAZING METHODS

To further verify the superiority of the proposed method, for the synthetic hazy images, objective indicators such as the peak-signal-to-noise-ratio (PSNR), SSIM, information entropy (IE) and average gradient (AG) are used to evaluate each method in synthetic hazy images. The larger the PSNR, the smaller the difference between the two images. The larger the SSIM, the higher the structural similarity between the two images. The larger the IE, the more the average information the image carries. The larger the AG, the higher the definition of the image. For the real hazy images, since there is no corresponding contrast image, only IE and AG of the dehazed image are calculated.

As shown in Table 1, for synthetic hazy image test set, the dehazing results of the proposed method achieve a certain degree of lead in terms of PSNR, SSIM, IE and AG. As shown in Table 2 and Table 3, for real hazy image test sets, the results of the proposed method are improved in IE and AG. In addition, the improvement of IE is more obvious and the proposed method has better generalization.

D. INFLUENCE OF K AND LOSS FUNCTIONS

To analyze the effects of K and loss functions on the image dehazing results, $K+L_a$, $K+L_a+L1^*$, $K+L_a+L_{SSIM}+L1^*$ and $L_a+L_{SSIM}+L1^*$ in the network are compared in the synthetic hazy image test set under different epochs. As shown in Figure 7, when epoch ≥ 75 and $K+L_a+L_{SSIM}+L1^*$ is in the network, the final dehazing results are better than the others in PSNR, SSIM, IE and AG.

V. CONCLUSION

In this paper, a new end-to-end dehazing network is proposed. The network uses U-net to generate the composed image K which is jointly estimated by transmission map t and atmospheric light value A. Next, dehazed image is obtained by the improved atmospheric scattering model. Besides, training the whole network through CGAN. In addition, SSIM is added to the loss function of the network to increase image details. The dehazing results of the proposed method show good performance in both subjective visual effects and objective indicators. Moreover, it has good generalization. The experimental results show that the proposed method can remove haze better and retain more image details.

REFERENCES

[1] Z. Liu, B. Xiao, M. Alrabeiah, K. Wang, and J. Chen, "Single image dehazing with a generic model-agnostic convolutional neural network," *IEEE Signal Process. Lett.*, vol. 26, no. 6, pp. 833–837, Jun. 2019.

[2] W. Ren, L. Ma, J. Zhang, J. Pan, X. Cao, W. Liu, and M.-H. Yang, "Gated fusion network for single image dehazing," in *Proc. IEEE/CVF Conf. Comput. Vis. Pattern Recognit.*, Salt Lake City, UT, USA, Jun. 2018, pp. 3253–3261.

[3] C. Wang, Z. Li, J. Wu, H. Fan, G. Xiao, and H. Zhang, "Deep residual haze network for image dehazing and deraining," *IEEE Access*, vol. 8, pp. 9488–9500, Jan. 2020.

[4] W. Wang, A. Wang, Q. Ai, C. Liu, and J. Liu, "AAGAN: Enhanced single image dehazing with attention-to-attention generative adversarial network," *IEEE Access*, vol. 7, pp. 173485–173498, 2019.

[5] L. Shen, Y. Zhao, Q. Peng, J. C.-W. Chan, and S. G. Kong, "An iterative image dehazing method with polarization," *IEEE Trans. Multimedia*, vol. 21, no. 5, pp. 1093–1107, May 2019.

[6] Q. Wu, W. Ren, and X. Cao, "Learning interleaved cascade of shrinkage fields for joint image dehazing and denoising," *IEEE Trans. Image Process.*, vol. 29, pp. 1788–1801, Sep. 2020.

[7] K. He, J. Sun, and X. Tang, "Single image haze removal using dark channel prior," *IEEE Trans. Pattern Anal. Mach. Intell.*, vol. 33, no. 12, pp. 2341–2353, Dec. 2011.

[8] K. He, J. Sun, and X. Tang, "Guided image filtering," *IEEE Trans. Pattern Anal. Mach. Intell.*, vol. 35, no. 6, pp. 1397–1409, Jun. 2013.

[9] C. O. Ancuti and C. Ancuti, "Single image dehazing by multi-scale fusion," *IEEE Trans. Image Process.*, vol. 22, no. 8, pp. 3271–3282, Aug. 2013.

[10] D. Berman, T. Treibitz, and S. Avidan, "Non-local image dehazing," in *Proc. IEEE Conf. Comput. Vis. Pattern Recognit. (CVPR)*, Las Vegas, NV, USA, Jun. 2016, pp. 1674–1682.

[11] B. Cai, X. Xu, K. Jia, C. Qing, and D. Tao, "DehazeNet: An end-to-end system for single image haze removal," *IEEE Trans. Image Process.*, vol. 25, no. 11, pp. 5187–5198, Nov. 2016.

[12] W. Ren, S. Liu, H. Zhuang, J. Pan, X. Cao, and M. Yang, "Single image dehazing via multi-scale convolutional neural networks," in *Proc. ECCV*, Amsterdam, The Netherlands, Oct. 2016, pp. 154–169.

[13] R. Li, J. Pan, Z. Li, and J. Tang, "Single image dehazing via conditional generative adversarial network," in *Proc. IEEE/CVF Conf. Comput. Vis. Pattern Recognit.*, Salt Lake City, UT, USA, Jun. 2018, pp. 8202–8211.

[14] M. Mirza and S. Osindero, "Conditional generative adversarial nets," 2014, *arXiv:1411.1784*. [Online]. Available: http://arxiv.org/abs/1411.1784

[15] D. Engin, A. Genc, and H. K. Ekenel, "Cycle-dehaze: Enhanced CycleGAN for single image dehazing," in *Proc. IEEE/CVF Conf. Comput. Vis. Pattern Recognit. Workshops (CVPRW)*, Salt Lake City, UT, USA, Jun. 2018, pp. 825–833.

[16] B. Li, X. Peng, Z. Wang, J. Xu, and D. Feng, "AOD-Net: All-in-one dehazing network," in *Proc. IEEE Int. Conf. Comput. Vis. (ICCV)*, Venice, Italy, Oct. 2017, pp. 4770–4778.

[17] H. Zhao, O. Gallo, I. Frosio, and J. Kautz, "Loss functions for image restoration with neural networks," *IEEE Trans. Comput. Imag.*, vol. 3, no. 1, pp. 47–57, Mar. 2017.

[18] S. G. Narasimhan and S. K. Nayar, "Chromatic framework for vision in bad weather," in *Proc. IEEE Conf. Comput. Vis. Pattern Recognit. (CVPR)*, Hilton Head Island, SC, USA, Jun. 2000, pp. 598–605.

[19] S. G. Narasimhan and S. K. Nayar, "Vision and the atmosphere," *Int. J. Comput. Vis.*, vol. 48, no. 3, pp. 233–254, Jul. 2002.

[20] I. Goodfellow, J. Pouget-Abadie, M. Mirza, B. Xu, D. Warde-Farley, S. Ozair, A. Courville, and Y. Bengio, "Generative adversarial nets," in *Proc. NIPS*, Montreal, QC, Canada, Dec. 2014, pp. 2672–2680.

[21] O. Ronneberger, P. Fischer, and T. Brox, "U-Net: Convolutional networks for biomedical image segmentation," in *Proc. MICCAI*, Munich, Germany, Oct. 2015, pp. 234–241.

[22] B. Li, W. Ren, D. Fu, D. Tao, D. Feng, W. Zeng, and Z. Wang, "Benchmarking single-image dehazing and beyond," *IEEE Trans. Image Process.*, vol. 28, no. 1, pp. 492–505, Jan. 2019.

[23] D. Scharstein, "High-resolution stereo datasets with subpixel-accurate ground truth," in *Proc. GCPR*, Münster, Germany, Sep. 2014, pp. 31–42.

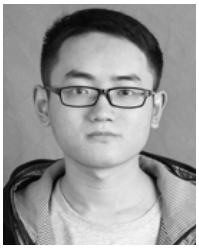

KAILEI GAN is currently pursuing the M.S. degree with the Faculty of Electrical Engineering and Computer Science, Ningbo University. His main research interests include computer image processing, computer vision, and machine learning.

JIEYU ZHAO received the B.S. and M.S. degrees in computer science from Zhejiang University, Hangzhou, China, in 1985 and 1988, respectively, and the Ph.D. degree in computer science from the Royal Holloway, University of London, Egham, U.K., in 1995. He is currently a Full Professor with Ningbo University, Ningbo, China. His current research interests include deep learning, computer vision, and neural networks.

HAO CHEN is currently pursuing the Ph.D. degree with the Faculty of Electrical Engineering and Computer Science, Ningbo University. His main research interests include 3D reconstruction, pattern recognition, and machine learning.